ACS Biomaterials SCIENCE & ENGINEERING

pubs.acs.org/journal/abseba

Methods/Protocols

Microfluidic Systems For Manufacturing of Microparticle-Based Drug-Delivery Systems: Design, Construction, and Operation

Nihan Yonet-Tanyeri, Maher Amer, Stephen C. Balmert, Emrullah Korkmaz, Louis D. Falo, Jr., and Steven R. Little*

Cite This: *ACS Biomater. Sci. Eng.* 2022, 8, 2864–2877

Read Online

ACCESS | Metrics & More | Article Recommendations | Supporting Information

ABSTRACT: Particles synthesized from biodegradable polymers hold great potential as controlled drug delivery systems. Continuous flow platforms based on microfluidics offer attractive advantages over conventional batch-emulsification techniques for the scalable fabrication of drug-loaded particles with controlled physicochemical properties. However, widespread utilization of microfluidic technologies for the manufacturing of drug-loaded particles has been hindered largely by the lack of practical guidelines toward cost-effective development and reliable operation of microfluidic systems. Here, we present a framework for rational design and construction of microfluidic systems using commercially available components for high-throughput production of uniform biodegradable particles encapsulating drugs. We also demonstrate successful implementation of this framework to devise a robust microfluidic system that is capable of producing drug-carrying particles with desired characteristics. The guidelines provided in this study will likely help broaden the applicability of microfluidic technologies for the synthesis of high-quality, drug-loaded biodegradable particles.

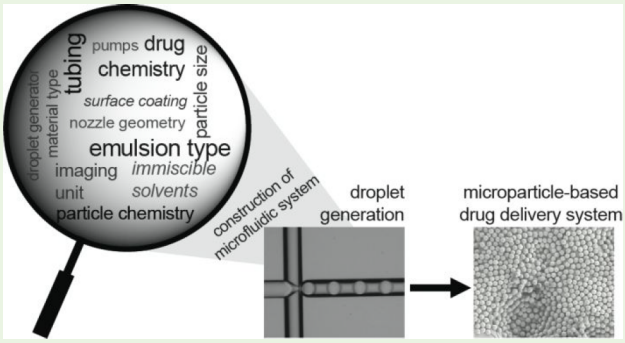

KEYWORDS: *microfluidics, droplet generators, biodegradable microparticles, drug carriers, PLGA*

INTRODUCTION

Microfluidic technology represents a powerful tool for the fabrication of particle-based drug delivery systems. Notably, batch processes, used for producing microencapsulated drugs, require large volumes of solvent and result in significant batch-to-batch variations in physical characteristics and drug-release profiles.[1−4] In contrast, microfluidic approaches enable precise control over fluid flow and mixing at the nanoliter scale within microchannels to produce uniform droplets that can be further solidified to form well-defined, drug-carrying particles.[5−7] Further, centrifugal and capillary-based microfluidics can generate sophisticated and versatile microcarriers that are impractical to produce with common microfluidic methods.[8−11] Thus, microfluidic approaches can minimize the batch-to-batch variation of the drug carriers, leading to better reproducibility and control over particle characteristics.[12,13]

Synthesis of particle-based drug carriers using microfluidic technology is typically carried out by encapsulating active pharmaceutical ingredients (APIs) in discrete droplets. The liquid medium containing the drug molecules and the carrier is dispersed into an immiscible continuous phase within a microfluidic droplet generator. By controlling microfluidic channel geometry and relative flow rates of the continuous and dispersed phases, highly monodisperse droplets with sizes ranging from 1 to 100 μm are generated and subsequently converted into microparticles using numerous cross-linking or solidification approaches.[14−17] Further, the composition of droplets, especially in the context of emulsion type, can be altered by tailoring such device configurations.[18] This allows for the development of particle-based drug delivery systems with tunable physicochemical properties and, in turn, predictable and tunable release characteristics.

Tailor-made microfluidic devices or droplet generators, created using advanced microfabrication techniques, have been successfully implemented for the production of particle-based drug delivery systems. However, the high cost, ramp-up time, and complexity of these microfabrication methods have limited the rapid, cost-effective development of microfluidic devices and, in turn, the broad utility of microfluidic technology for scalable manufacturing of drug-loaded particles. Toward enabling widespread utilization of microfluidic technology, in the past decade several companies introduced prototyping services for microfluidic devices, and a number of microfluidic

Received: January 18, 2022
Accepted: May 24, 2022
Published: June 8, 2022

https://doi.org/10.1021/acsbiomaterials.2c00066
ACS Biomater. Sci. Eng. 2022, 8, 2864−2877

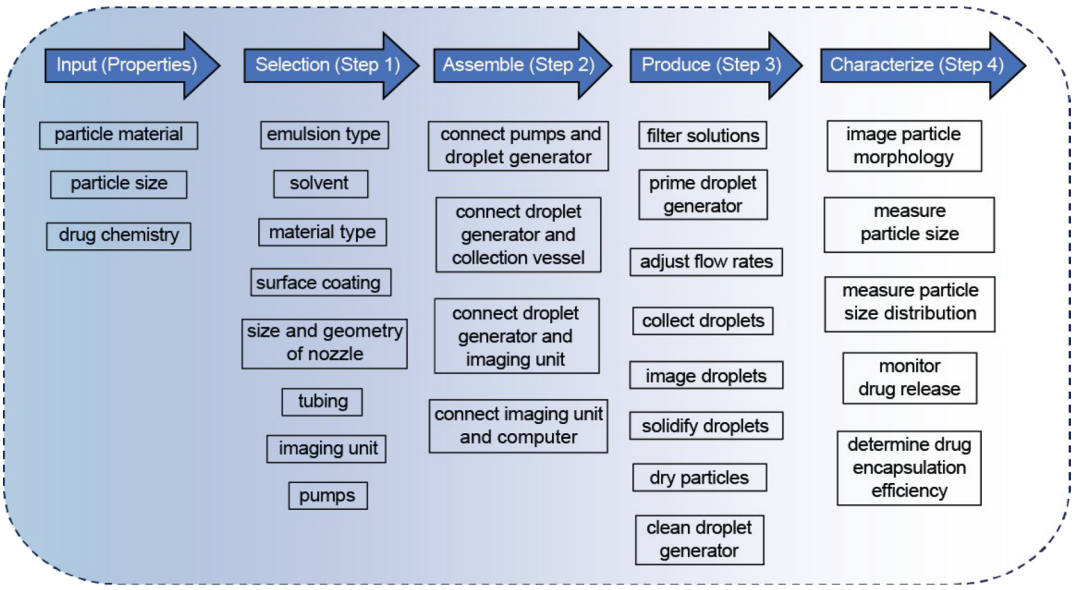

Figure 1. Framework to enable construction of a microfluidic system using commercially available components for the production of particle-based drug carriers.

platforms became commercially available.[19] Despite this exciting progress, application-driven selection of these microfluidic devices poses considerable challenges. This is exacerbated because these microfluidic devices also need to be used with suitable accessories and peripherals, such as connectors, tubing, and pumps, and *in situ* process characterization systems, including sensors and image acquisition setups, to enable cost-effective development of robust microfluidic systems that can be operated in a reliable and continuous fashion. Here, we provide practical guidelines to facilitate rational development of microfluidic systems using commercially available components to enable reproducible production of uniform microparticle-based drug carriers. We discuss selection criteria for chemical compatibility and particle composition, as well as the assembly of a representative microfluidic platform. Ultimately, we demonstrate the use of this platform to produce particle-based drug delivery systems using an FDA-approved biodegradable polymeric drug carrier, poly(L-lactide-*co*-glycolide) (PLGA), to encapsulate an FDA-approved drug, rapamycin.[20−25]

MATERIALS

Reagents. The following reagents were used for droplet generation: Resomer RG 502H poly(L-lactide-*co*-glycolide) (PLGA) (Sigma-Aldrich 719897), dichloromethane (Sigma-Aldrich 32222), aqua phase (Dolomite P/N 3200775), poly(vinyl alcohol) (Sigma-Aldrich 563900), helium gas, rapamycin (Alpha Esar J62473), dimethyl sulfoxide (DMSO) (Fisher Scientific D-128), and deionized distilled water (Milli-Q, Millipore). Reagents used for particle characterization are as follows: acetonitrile (Fisher Chemical A998-1), conductive carbon or copper type (Ted Pella), and liquid nitrogen.

Equipment. General equipment used includes a lab coat, gloves, and safety goggles. The following were used for droplet and particle generation: 3D flow-focusing droplet generator with a hydrophilic and elliptical channel with 100 × 105 μm dimensions (Dolomite 3200433); pressure pumps (Dolomite Mitos 3200175); flow sensor (30−1000 μL/min) (Dolomite Mitos 3200097); flow sensor (1−50 μL/min) (Dolomite Mitos 3200098) with a converter (Dolomite 3200285); chip interface H (Dolomite 3000155); 4-way linear connector (Dolomite 3000024); tubing starter pack including polytetrafluoroethylene (PTFE) tubing with 250 μm inner diameter, 1/16 in. outer diameter (Dolomite 3000415), 1/4 in.-28 fluid fittings (Dolomite 3200588), and 1/4 in.-28 straight female coupling, ethylene chlorotrifluoroethylene (ECTFE) (Dolomite 3000399); linear connector 4-way (Dolomite 3000024); ethylene tetrafluoroethylene (ETFE) T-connector (Dolomite 3000397); ferrule with integrated filter (Dolomite 3200245); Frit in Ferr (IDEX Health & Science SS/PCTFE P-272); female luer−female union 1/8 (Thermo Scientific P628); plug 1.6 mm (Blacktrace 3000056); sensor interface (Dolomite 3200200); end fittings and ferrules for 1.6 mm tubing (Dolomite 30000477); 2-way in-line valve (Dolomite 3200087); trinocular compound microscope with 10× objective (40×−1000× LED Siedentopf); high-speed microscope camera (Pixelink M5C-CYL) and its software (Pixelink); adapter converting photo port to C-mount (AmScope CPC); flow-control center (FCC) software (Dolomite 4.1.9 free version); pressure regulator for helium gas (Miller−Smith 580 CGA inlet connection, helium welding regulator); air filter (Husky HAD70603AV 3/8 in. standard poly bowl air filter); pressure regulator before connection to pressure pumps (Husky HDA72200 3/8 in. high-performance air regulator); 4-way gas manifold to split the gas line; pneumatic connector kit (Dolomite 3200034); lab balance (0.0001 g sensitivity); rubber-free syringes (5 and 10 mL); syringe needles (18G); 0.2 μm and 30 mm PTFE disposable syringe filters (Whatman WHA10463503); 0.2 μm PES syringe filters (Whatman WHA67802502); clear glass vials (1 dram−3.7 mL, 20 mL); magnetic stir bar (1 cm); vortex mixer (Fisher Scientific); temperature-controlled oil bath with stir plate; lab refrigerator; centrifuge (Thermofisher Sorvall Legend XIR); lyophilizer (VirTis Benchtop K); falcon tubes, 50 mL; homogenizer (Silverson L4RT-A); timer; and ImageJ Software.

The following pieces of equipment were used for particle characterization: scanning electron microscope (Zeiss Sigma VP); sputter coater (Denton Desk V); Eppendorf tubes (Protein LoBind tube 1.5 mL); pipettes, 100 and 1000 μL (Eppendorf); 96-well clear flat bottom plate (Corning Costar 3697); and microplate reader (SpectraMax M5). Additionally, MATLAB software was utilized.

METHODS

The general framework for design, construction, and operation of a microfluidic system to produce microparticle-based drug carriers includes four steps (Figure 1). Step 1 is the selection of microfluidic system components, such as the droplet generator, fluidic pumps, tubing with connection accessories, and imaging unit. The selection of these components is heavily dependent on the given input information, particle material type, desired particle size, and chemistry of the drug. Step 2 is the assembly of these components. Step 3 is the operational

https://doi.org/10.1021/acsbiomaterials.2c00066
ACS Biomater. Sci. Eng. 2022, 8, 2864−2877

Table 1. Biodegradable Polymers for Emulsion-Based Microparticle Production and Possible Solvent Options[a,b]

drug carrier	common solvents	representative drug/polymer combination	emulsion type	solvent combination	ref
hydrophobic					
PLGA	DCM, ethyl acetate, acetone, THF	indomethacin[c]/PLGA	O/W	DCM/water	37
PLA	dioxane, acetonitrile, chloroform, DCM, 1,1,2-TCA, dichloroacetic acid	glucagon-like peptide-1[d]/PLA	W/O/W	water/DCM/water	36
PCL	DMF, DCM, TFE, chloroform	levobunolol[e]/PCL	W/O/W	water/DCM/water	34
hydrophilic					
alginate	water	VEGF[f]/alginate	W/O	water/iso-octane	32
chitosan	aqueous acetic acid solution	resveratrol[c]/chitosan	W/O	acetic acid solution/liquid paraffin	31
gelatin	water	ciprofloxacin[e]/acidic gelatin	W/O	water/olive oil	33
hyaluronic acid	water	progesterone[g]/hyaluronic acid	O/W/O	sunflower oil/water/soybean oil	39
carboxymethyl cellulose	water	cranberry extract[h]/carboxymethyl cellulose	W/O	water/liquid paraffin	35

[a]A representative drug/polymer/solvent combination and emulsion type for each polymer type is listed. [b]PLGA, poly(L-lactide-*co*-glycolide); PLA, poly(lactic acid); PCL, poly(ε-caprolactone); DCM, dichloromethane; THF, tetrahydrofuran; DMF, dimethylformamide; 1,1,2-TCA, 1,1,2-trichloroethane; TFE, 2,2,2-trifluoroethanol. [c]Hydrophobic small molecule. [d]Peptide. [e]Hydrophilic small molecule. [f]Protein. [g]Lipophilic steroid. [h]Hydrophilic mix of natural extract.

procedure for droplet generation and subsequent particle formation in a post-droplet production process. Step 4 is the particle characterization in regards to size, size distribution, and morphology of the particles, as well as drug encapsulation efficiency. Additionally, microparticles can be further characterized for *in vitro* release kinetics by already established quality-control protocols used in clinical applications to represent the *in vitro*−*in vivo* correlation.[26,27]

Procedure Overview. An overview of the procedure is detailed here:

- Step 1: Selection of the system components.
- Step 2: Assembly of the microfluidic setup.
- Step 3: Operation of the microfluidic setup for droplet and particle production.
- Step 4: Characterization of the particles.

Step 1: Selection of the System Components. A microfluidic setup is a multicomponent system, including a droplet generator, fluid pumps, accessories that provide connections among the droplet generator and pumps, and an imaging unit. In this section, we highlight critical design parameters that should be considered when selecting suitable commercial products for these four components to produce particle-based drug carriers. Further, we describe operational aspects of a representative microfluidic setup to demonstrate the production of a drug carrier example: a hydrophobic drug, rapamycin, encapsulated in polymer-based (PLGA) microparticles.

There are three important features that will directly impact the selection of an adequate commercial droplet generator. One of these features is the material type of the commercial droplet generator. Given that a number of different material types are available for commercial droplet generators such as polydimethylsiloxane (PDMS), polycarbonate (PC), poly(methyl methacrylate) (PMMA), cyclic olefin copolymer (COC), and glass, it is necessary to initially determine the emulsion type (single or double), identify the immiscible fluids, and finally select a droplet generator that is compatible with the fluids of choice. The type of emulsion that is intended to be produced depends on the chemical feature of the drug carrier (i.e., polymer) and the drug itself. For instance, hydrophilic drugs (e.g., proteins, peptides, or small molecules) can be encapsulated in hydrophilic drug carriers, such as carboxymethyl cellulose, alginate, gelatin, or chitosan, via generation of water-in-oil (W/O) emulsions, while water-in-oil-in-water (W/O/W) emulsions are necessary for the encapsulation of hydrophilic drugs in hydrophobic drug carriers, such as PLGA, poly(lactic acid) (PLA), or poly(ε-caprolactone) (PCL).[21,28−36] If both the drug carrier and drug are hydrophobic (e.g., small molecules) and exhibit good solubility in a common organic solvent, an oil-in-water (O/W) emulsion will be suitable for hydrophobic drug encapsulation.[37,38] In addition, hydrophobic drugs can be encapsulated in hydrophilic drug carriers such as hyaluronic acid by oil-in-water-in-oil emulsions (O/W/O).[39] Table 1 lists most widely used biodegradable polymers for emulsion-based microparticle production including the common solvents and a representative drug/polymer/solvent combination with corresponding emulsion type for each polymer type. On the basis of the immiscible fluids to be used, the most compatible material for the droplet generator can be selected accordingly.

Even though surfactants are not directly linked to the selection process for an adequate commercial droplet generator, especially when the material compatibility is considered, it is important to briefly discuss their role in droplet production using microfluidic systems. Surfactants usually refer to amphiphilic molecules that can show affinities to two different immiscible solvent phases. Given this amphiphilicity, surfactant molecules localize at the interface between immiscible phases, reducing the surface tension between the liquids.[40] In this context, surfactants can significantly affect droplet formation and droplet stability.[41] Usually, higher surfactant concentration in the continuous phase tends to reduce the droplet size.[42,43] The selection of surfactant and optimum surfactant concentration depend on the specific droplet formulation that is desired. Therefore, we refer to previous reviews for further discussion on surfactants for microfluidic-assisted droplet production.[44,45]

Generally, chemical resistance of polymeric droplet generators to organic solvents is poor. For instance, halogenated hydrocarbons, ketones, aldehydes, esters, amines, and aromatics are not recommended for PC droplet generators. Alcohols, esters, ketones, concentrated acids and bases, halogenated hydrocarbons, and aromatics are not compatible with PMMA devices.[46] Similarly, halogenated hydrocarbons, amines, and aromatics are not suggested for PDMS-based droplet generators.[47] COC droplet generators, as the most resistant polymeric devices, are not compatible with nonpolar solvents, mineral oils (hydrocarbons), and halogenated hydrocarbons.[46] If one of these solvents is required for droplet formation, chemically resistant glass droplet generators would be the best option. In addition to the solvent resistance of the commercial droplet generators, the choice of the emulsion type may require additional chemical treatment on the surface of the microfluidic channels. Such treatments can alter the surface chemistry of the microfluidic channels to create a hydrophobic coating that assists in maintaining the wettability of the channels with the continuous phase and thus stabilizing droplets and minimizing droplet coalescence in the continuous phase. In this regard, the hydrophobic coating is critical, regardless of the droplet generator material, for emulsions with hydrophobic organic solvents used for the continuous phase (e.g., W/O emulsions).

In this report, the microfluidic setup was constructed for the encapsulation of a hydrophobic drug, rapamycin, in a hydrophobic

https://doi.org/10.1021/acsbiomaterials.2c00066
ACS Biomater. Sci. Eng. 2022, 8, 2864−2877

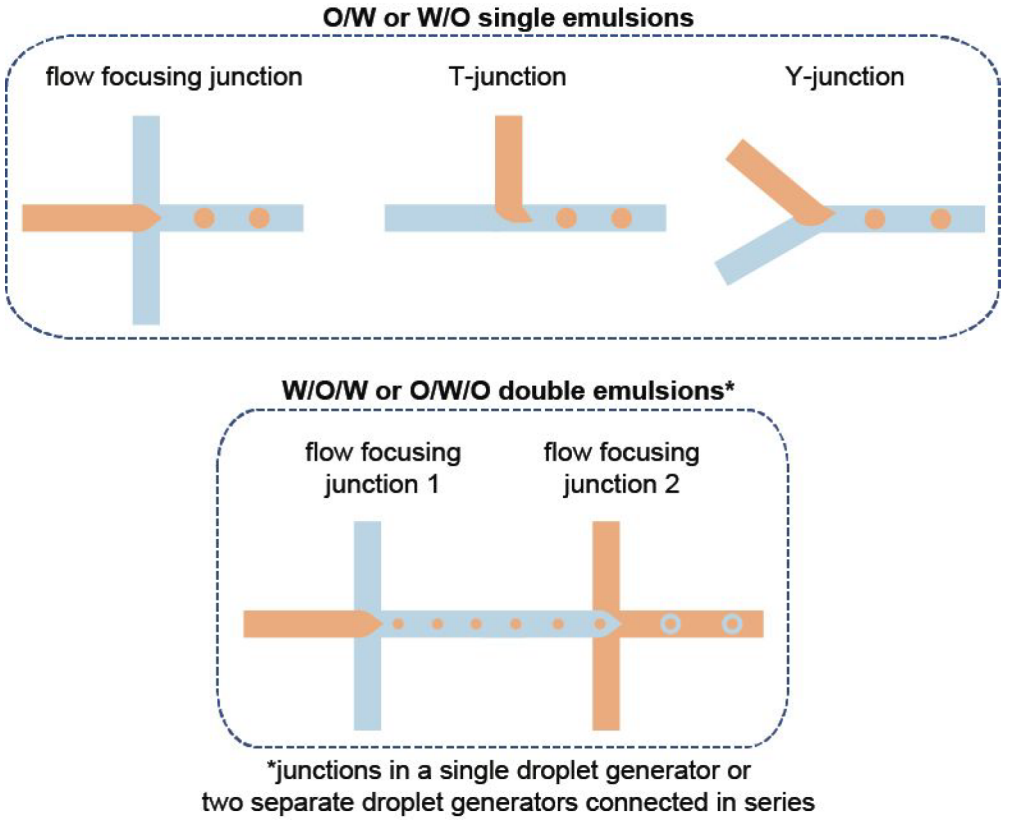

Figure 2. Summary of the design considerations to select the commercially available droplet generator based on the droplet generator configurations to create different types of emulsions.

polymer carrier, PLGA, by generating O/W single emulsions. Rapamycin and PLGA are both soluble in dichloromethane (DCM). Therefore, a DCM solution of rapamycin and PLGA was used as the dispersed phase, one of the immiscible fluids for the droplet production. Water was selected as the continuous phase due to its immiscibility with DCM, and surfactant was included to stabilize the emulsion. Because the commercial polymeric droplet generators have poor chemical compatibility with DCM, a glass device was used to generate O/W PLGA droplets.

The other two key parameters of the selection criteria for a commercial droplet generator are associated with the configurational aspect of the device, such as size and geometry of the nozzle where the droplets are formed. The target droplet size is directly linked with the size of the nozzle even though other parameters, including the drug carrier concentration and flow rates of dispersed and continuous phases, are known to affect the droplet size. In this regard, most droplet generator providers specify the range of droplet sizes that a specific droplet generator can produce. Therefore, it will be suitable to select the nozzle size that fits within the range of anticipated droplet size. On the other hand, nozzle geometry plays a significant role in the production of double- or higher-order emulsions, and more complex device configurations such as multiple flow focusing nozzles are required (Figure 2). Notably, some of the droplet generator providers support customer services that can arrange custom-designed products. The customization of a commercial droplet generator can involve various adjustments to size and geometry of the nozzle, surface treatment, and flexibility in the number of droplet generating junctions that work either independently or simultaneously in a single device. In the data described herein, a glass-type commercial droplet generator with a 100 μm wide and 105 μm long elliptical channel and a flow focusing nozzle configuration was selected for the production of PLGA microparticles.

The second essential component in a microfluidic setup is the fluid control system used to pump the immiscible fluids from reservoirs toward the droplet generator. There are two types of commercially available pumping devices that are adaptable to microfluidic systems: syringe and pressure pumps. To make a selection between these two types of pumps, it will be helpful to consider the total liquid volume to be pumped into the droplet generator, the required flow stability, and the response time upon switching to a new flow rate.[48] The reservoirs for the operating fluids are conventional disposable syringes for syringe pumps. Therefore, the total liquid volume for droplet production depends on the size of the syringe with which a syringe pump is compatible. Currently, syringe pumps can work with different-sized syringes so that the reservoir volume can range from 1 to 100 mL. However, syringe pumps exhibit two major issues that may impact the droplet size distribution: instability of the flow rate, especially at low flow rates with larger diameter syringes, and slow response times when switching to a new flow rate.[49]

Pressure pumps perform slightly differently than syringe pumps. For instance, more stable flow rates can be achieved using pressure pumps, which apply pressure from a compressed air or inert gas supply onto a sealed fluid reservoir.[50] Moreover, pressure pumps have a faster response time due to a closed-loop flow control. However, the need for an external flow sensor/controller connected to each pressure pump to measure and control the flow could be considered an economical disadvantage due to additional cost to the pumping system.

Regarding the total liquid volume, the volume of the operating fluid is defined by the pressure pump design, which may be unique to the product. Some products are connected to an external liquid reservoir, such as falcon tube or bottles, via specialized tubing connectors. This product design allows for the maximum operating fluid volume to expand larger than 100 mL. There are other pressure pump designs that come with a built-in pressure chamber to store the fluid container. In such products, the maximum operating liquid volume is limited by the fixed volume of the built-in reservoir. Generally, the mobility of each immiscible fluid from external reservoirs is controlled by an assigned pressure pump. However, it is also possible to drive two immiscible fluids from separate external reservoirs to produce ultramonodisperse droplets using a single pressure pump and a special device configuration.[51] In this work, pressure-driven pumping devices with

https://doi.org/10.1021/acsbiomaterials.2c00066
ACS Biomater. Sci. Eng. 2022, 8, 2864−2877

Table 2. Summary of the Selection Criteria for Microfluidic System Components Including Fluid Control Systems and Tubing[a]

	selection criteria				
system components	operating liquid volume	fluid flow characteristics	material type	chemical resistance	dimension
fluid-control system					
syringe pumps	1−100 mL	less stable flow rate, slow response time			
pressure pumps	10 mL−1 L	stable flow rate, fast response time			
with external fluid reservoir	10−1 mL				
with built-in reservoir	20 mL				
tubing			PEEK, PTFE, FEP, ETFE, Tygon, silicone	PEEK not recommended for DCM, THF, or DMSO	i.d. = 25 μm−3 mm, o.d. = 1−6.4 mm

[a]PEEK, polyetheretherketone; PTFE, polytetrafluoroethylene; FEP, fluorinated ethylene propylene; ETFE, ethylene tetrafluoroethylene; i.d., inner diameter; o.d., outer diameter.

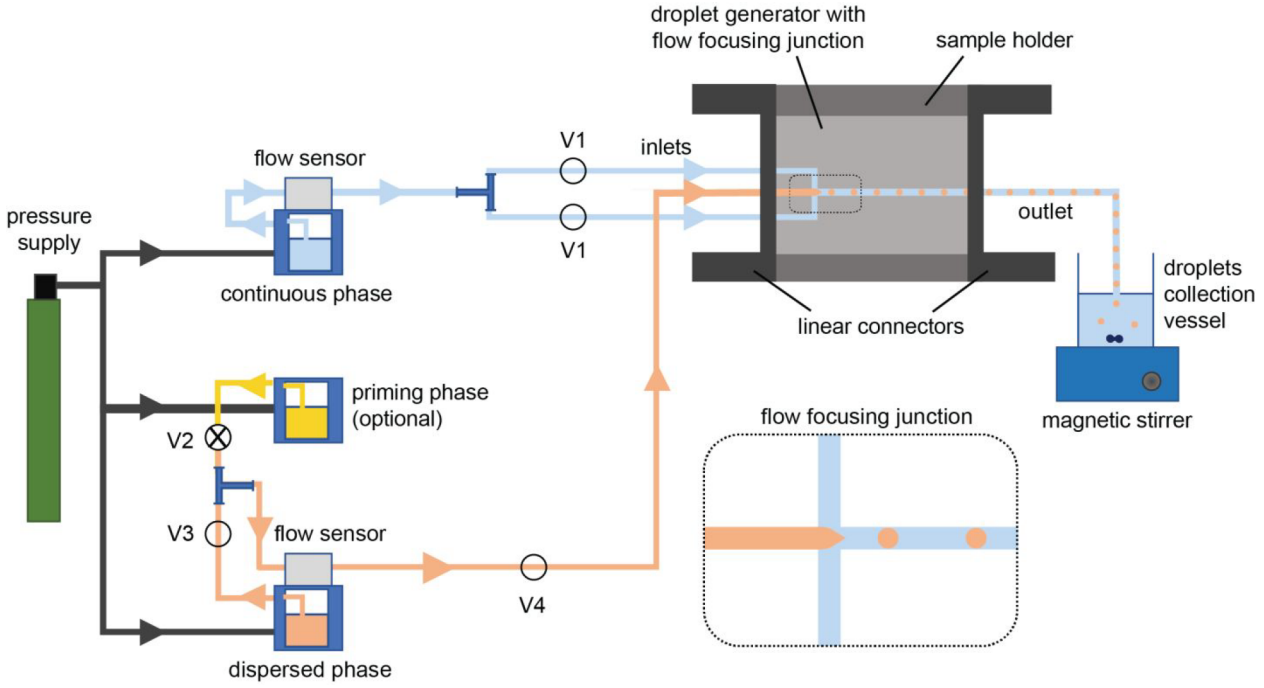

Figure 3. Schematic illustration of a representative microfluidic setup depicts the essential connections to a droplet generator to produce O/W or W/O emulsions. In this setup, pressure-driven pumping devices, as the example of a fluid flow system, are included where pressure supply and flow sensors are the necessary components. This microfluidic setup also incorporates some optional system components such as a priming pump and manual valves (V1−V4).

built-in reservoirs were used to drive the dispersed and continuous phases into the droplet generator.

The third component of a microfluidic setup is the connection accessories, including tubing for fluid transportation, connectors, and fittings that are adaptable for the selected droplet generator. A number of different tubing options are available based on the material type and dimension of the tubing inner and outer diameters. Some of the most commonly used tubing materials include polyetheretherketone (PEEK), polytetrafluoroethylene (PTFE), fluorinated ethylene propylene (FEP), ethylene tetrafluoroethylene (ETFE), Tygon, and silicone. PEEK tubing is not recommended if the operating fluid is DCM, THF, or DMSO due to solvent-induced swelling of the tubing.[52] PTFE, FEP, and ETFE are chemically resistant to most solvents. PTFE and FEP usually work well under low pressure, while ETFE is used in medium pressure.[52] Regardless of the material type, microfluidic tubing can deform under very slow flow rate applications, leading to pressure instability along the tubing. To reduce this effect, tubing with a small inner diameter and rigid structure should be selected for more consistent pressure in the tubing. In addition to the tubing material, there are several tubing options that have various inner and outer diameters. Generally, the tubing inner and outer diameters are 0.5 and 1.6 mm, respectively. However, it is possible to find products with inner diameters ranging from 25 μm to 3 mm, while the outer diameters range from 1 to 6.4 mm. Table 2 summarizes the overall selection criteria for microfluidic system components, specifically for the fluid control systems and tubing. For the method described herein, we have selected the PTFE tubing with an inner diameter of 250 μm.

Similar to microfluidic tubing, tubing connectors, fittings, and valves should be not only chemically resistant but also a reliable junction for maintaining a leak-free fluid flow. These connectors are localized between soft elements, for instance, connecting two tubing lines. Also, these connectors necessarily bring rigid elements and soft elements together throughout the microfluidic system. Such connectors are typically used in between the chip and tubing or pumps and tubing.

https://doi.org/10.1021/acsbiomaterials.2c00066
ACS Biomater. Sci. Eng. 2022, 8, 2864−2877

Especially when a high-pressure flow condition is considered, the utmost leak-free performance of these junction becomes very critical for a microfluidic system.

The fourth and final component of a microfluidic setup is the imaging unit that will enable in situ monitoring of fluid flow, the droplet formation at the nozzle, and any issues with clogging that may occur at the nozzle or in other parts of the droplet generator. In this context, computer-assisted imaging of individual droplets may be helpful for further analysis to correlate the droplet size with the size of the microparticles. Imaging the individual droplets requires the use of a high-speed camera with sufficiently high frame rate (as high as 25 000 frames/s) that also reduces the image blur caused by long exposure times and moving droplets.[53] However, a high-speed camera is relatively more expensive as compared to a common digital microscope camera that can still function to monitor in situ flow of fluids and clogging issues to some degree. In this work, a high-speed camera with 5 MP resolution and frame rates of up to 815 frames/s was connected to a trinocular upright microscope for imaging purposes.

Step 2: Assembly of the Microfluidic Setup. The assembly of the microfluidic components may be slightly different for each microfluidic setup due to the modularity of these systems and the product specifications that may vary for each vendor; however, the overall goal is to build a leakage-free fluid flow that will operate under desired flow conditions for droplet production. Because the microfluidic setup we used herein is one of the application packages provided by a single vendor, we refer to the supporting documents for the vendor's listed assembly instruction.[54] In this section, we highlight common aspects of the assembly of a microfluidic setup, which would apply to various commercially available systems.

Connecting the Droplet Generator to the Flow Control System and the Droplet Collection Vessel. The fluid control system (syringe or pressure pumps) is connected to the droplet generator via an appropriate number of tubing inlets, depending on the device configuration. For example, a droplet generator with a flow focusing junction is connected to the corresponding pumps (dedicated to continuous and dispersed phases) with two tubing inlets for the continuous phase and one tubing inlet for the dispersed phase (Figure 3). Some device configurations may have one continuous phase inlet that later splits into two streams within the device. In that case, one tubing for the continuous phase inlet is used to connect the device to the respective pump. In the case of a Y-junction or a T-junction device configuration, the droplet generator needs a single tubing inlet for each phase for the connection with the pumps. If the droplet generator has more than one junction, especially for the production of double- or higher-order emulsions (Figure 2), additional tubing may be necessary to feed the droplet generator. Finally, depending on the number of outlets in the droplet generator, the necessary tubing pieces are attached to the droplet generator to provide the connection to a droplet collection vessel.

When establishing the connections between the droplet generator and the fluid-control system, a device holder may be necessary to maintain a leak-free fluid flow by securing a tight tubing connection with the droplet generator. For example, though less common, droplet generators with side connections require custom-designed holders with in-line connectors on each side (Figure 3). Droplet generators with top surface connections, more common among commercial devices, are compatible with another custom-designed holder type where the inlet and outlet tubings are aligned perpendicular to the device top surface and pass through holes on the top piece of the device holder. On the other hand, it is possible to set up a microfluidic system without using a device holder. In this case, the microfluidic setup should include a droplet generator that has either top inlets and outlets wide enough to directly fit tubing or integrated luers that allow for securing the luer lock-supported tubing connections.

Some of the connection pieces in the microfluidic setup are optional items and may bring further benefits for the users depending on the specific needs. In this regard, the tubing connections between the pumps and the droplet generator may be supported by a frit-in-a-ferrule at the threaded fitting site if the continuous or dispersed phase is intended to be filtered through the fluid flow line while the pumping system is running. The benefit of including this in-line fluid filtration ferrule in the microfluidic setup is to reduce the risks for possible clogging issues. Similarly, a bubble trap can be set in the fluid flow line to minimize the air bubble-associated fluctuation in the fluid flow rate. Moreover, users may consider fixing manual valves, another optional component, between the pumps and the droplet generator to improve the flow control. The use of manual one-way valves is especially critical if the microfluidic setup has backflow issues. Backflow occurs when fluids suddenly flow toward the reservoir and causes undesired mixing of continuous and dispersed phases. Further, an additional pump may be added to the microfluidic setup if users prefer to flush the droplet generator with the selected priming fluid between consecutive experiments. For this purpose, the fluid flow line is attached to another tubing using a T-connector to support the connection to the priming pump. A manual two-way valve in this connection site is necessary for switching fluid flow from the priming phase to the continuous phase (Figure 3).

Connecting the Computer-Aided Imaging System to the Microfluidic Setup. The computer-aided imaging system is composed of two subunits: a microscope and a camera. A trinocular bright-field microscope is an ideal imaging tool to monitor the fluid flow during the droplet generation and subsequent device cleaning process because binocular is used for manual monitoring of the droplet generator. In addition, a digital or microscope camera can be attached to the third ocular with an adapter that converts the microscope photo port to the C-mount version of a lens mount. Thus, digital images at the field of view are obtained from this camera using a supplier-provided software package and transported to a computer through a USB 3.0 locking cable connection. In this imaging system, a 10× objective lens offers an adequate view to observe the microfluidic channels and the droplet production. However, in the case of a small microfluidic channel less than 10 μm wide, a 20× objective lens would provide higher magnification on the field of view to monitor this channel.

Step 3: Operation of the Microfluidic Setup for Droplet and Particle Production. This section outlines a step-by-step description of polymer (PLGA) droplets production by using the microfluidic setup that was assembled based on the outline summarized in Figure 3.

Preparation of the Operating Fluids. To prepare the operating fluids, the steps below were followed:

(1) Eighty mg of polymer (PLGA) was dissolved in 4 mL of dichloromethane (DCM) to prepare 2% (w/v) solution in a 50 mL falcon tube. This solution was used in the droplet size measurements. For the hydrophobic drug encapsulation study, 200 mg of PLGA was dissolved in 4 mL of DCM to prepare 5% (w/v) solution, and this solution was mixed with 100 μL of rapamycin stock solution (10 mg/mL in DMSO).

(2) The PLGA solution was vortexed for 10 s for complete dissolution.

(3) The PLGA solution was filtered using a 0.2 μm PTFE syringe filter and collected in a dust-free glass vial, and its cap was kept tightly screwed to limit solvent evaporation.

(4) Twenty mL of the priming solution (DCM) was filtered through a PTFE syringe filter and collected in a dust-free glass vial, and its cap was screwed tightly.

Troubleshooting tips: (a) DCM can dissolve the rubber portion of the syringe plunge and the nylon component of regular nylon syringe filters. While filtering DCM and the PLGA solution, syringes with rubber-free plunges and PTFE syringe filters should be used. (b) DCM is a volatile organic solvent. To minimize its evaporation from the filtered PLGA solution, the glass vial's cap should be wrapped with paraffin until operation.

(5) Twenty mL of the continuous phase (aqua phase) was filtered by using a 0.2 μm PES syringe filter, and the filtered solution was collected in a dust-free glass vial.

Troubleshooting tip: Any dust or particulates that are present in the operating fluids (PLGA solution, DCM, or aqua phase) will likely result in clogging problems in the microchannels of the droplet generator. It is very important to store the filtered solutions in dust-free glass containers. Therefore, glass vials should be blown with pressurized air or nitrogen gas for 5−10 s before storing the filtered solutions.

https://doi.org/10.1021/acsbiomaterials.2c00066
ACS Biomater. Sci. Eng. 2022, 8, 2864−2877

(6) PVA (37 g) was dissolved in 925 mL of Milli-Q water to prepare a 4% (w/v) aqueous solution and stirred in an oil bath overnight at 37 °C. The PVA solution can be stored at 4 °C. Ten mL of diluted PVA solution (2% (w/v)) was used as the aqueous surfactant solution in the droplet collection vessel

Preparation of the External Pressure Supply, Pressure Pumps, and Imaging System. The steps for the preparation of the external pressure supply, pressure pumps, and imaging system are as follows:

(1) The valve of the helium gas tank was opened until the pressure level of the two-stage pressure regulator was set to 4 bar.

(2) The valve of the two-stage pressure regulator was opened to let the helium gas reach the pressure pumps. The maximum pressure level on the second pressure regulator should not exceed 4 bar.

(3) The pressure pumps were turned on, and then the FCC software was opened to connect the pressure pumps to the computer.

(4) The microscope was turned on, and the Pixelink software was opened to connect the live stream of the high-speed camera to the computer.

Production of Polymer Droplets. The production of polymer droplets uses the following steps.

(1) The glass vials filled with the operating solutions (aqua phase, DCM, and polymer (PLGA) in DCM) were placed into the chambers of the corresponding pressure pumps. For the production of drug encapsulating particles, the dispersed phase that was used included the drug (PLGA and rapamycin in DCM).

Troubleshooting tips: (a) Bubbles present in either the continuous or dispersed phase may cause flow rate instability and could result in variations in the droplet size. All solutions should be bubble-free before they are loaded in the pressure pump chambers. The use of inert gases, such as helium or argon, as the compressed pressure source may help reduce the bubble formation during the fluid flow process due to their limited solubility in water. (b) The tubing that is immersed in each operating fluid should be adjusted in such a way that it will be close to the bottom of the glass vial. As the fluid is consumed during the droplet production, the fluid level in the vial goes down. Keeping the tubing as close as possible to the bottom of the vial allows for maximization of the volume of the operating fluid pumped into the droplet generator, as well as of the time for the continuous fluid flow.

(2) The droplet generator was placed on the microscope stage, and the device was secured by taping it from two sides onto the microscope stage so that the device would stay steady during the droplet production process. Then the focus was adjusted at the flow focusing junction.

(3) The in-line valves V2 and V4 were in the open condition. The in-line valves V1 and V3 were kept closed.

(4) The outlet tubing was immersed in a waste container filled with water. The outlet tubing remained in the water until stable PLGA droplets at the desired flow rates or droplet size were maintained. Then, the waste was replaced with the PVA solution (2% (w/v)).

(5) The initial pressure levels of the three pressure pumps were seen in the FCC software. The pressure of the priming pump was increased up to 300 mbar to introduce the priming solution (DCM) to the droplet generator, and it was held until the microchannels were wetted.

(6) The pressure of the continuous phase pump was increased to 300 mbar, and then in-line valve V1 was opened.

(7) The pressure levels (up or down) were adjusted for both the priming and the continuous phase in order to form stable DCM droplets.

(8) The pressure of the dispersed phase pump was increased to the pressure level that was equivalent to the pressure level for the priming pump.

(9) In-line valve V2 was closed, and in-line valve V3 was quickly opened. This switched the dispersed phase from DCM to PLGA solution.

Critical point: The pressure level at which the stable droplets form depends on the hydrostatic pressure as the fluid volume in the chamber decreased. Therefore, the set pressure values for stable droplets formation may be different in each experiment if the initial fluid volumes are not the same. It is important to work within the pressure level with which the droplet generator is compatible. The droplet generator used in this study is resistant to a pressure level up to 3000 mbar.

(10) Ten minutes were allowed for the PLGA solution to be replaced with the priming solution, DCM, and for it to reach the droplet generator.

(11) The pressure control mode was switched to the flow-control mode on the FCC software for the continuous and dispersed phase pumps.

Critical point: The microfluidic system is initially run under the pressure control mode. However, as the fluid level in the chamber diminishes during the droplet production, the system adjusts itself to maintain the set pressure level in the chamber, which may result in fluctuations in the flow rate. Therefore, it is necessary to run the microfluidic system under the flow control mode where the flow rate will be kept constant throughout the droplet production.

(12) The waste container was replaced with a vial that was filled with 10 mL of PVA solution for the collection of PLGA droplets under mild stirring.

(13) The imaging software (Pixelink) setting was adjusted as follows to capture images of droplets if needed: exposure time, 0.001 ms; gain, 12.04 db; number of frames, 100; record time, 4.1 s; and playback option, 10 fs.

(14) If the size of the PLGA droplets was measured as a function of the flow rates, the flow rate of one phase was kept constant, the flow rate of the other phase was increased gradually, and images were taken. ImageJ was used to determine the droplet size. Eight images for each flow condition were used to determine the droplet size, and standard deviations were represented as the error.

(15) Collection of the polymer (in this case, PLGA) droplets continued, and the collection vial was replaced with a new one after 30 min of droplet collection. It should be noted that changing the collection vessel for a certain time interval will limit the droplet coalescence during the collection period. Droplet collection was continued in the second vial.

(16) Droplet collection was continued in the third and fourth vials for 30 min intervals, and the final vial was replaced with a waste vial once the droplet production was completed.

(17) The flow control mode was switched to the pressure control mode on the FCC software for each pump.

(18) The pressure level of the priming pump was adjusted with the pressure level of the dispersed phase pump.

(19) In-line valve V3 was closed, in-line valve V2 was quickly opened, and the flow for the dispersed phase pump was stopped.

(20) The priming and continuous phase pumps flowed for 10 min to wash any PLGA residue from the microfluidic setup.

(21) A vial of fresh DCM was placed in the dispersed phase pump, and the pressure level was adjusted with the priming pump. In-line valve V2 was closed and valve V3 was quickly opened so that fresh DCM washed the tubing for the dispersed phase pump. Then, the flow was stopped for the priming pump, and DCM was allowed to flow for 10 minutes.

(22) All in-line valves V1, V3, and V4 were closed. The dispersed phase and continuous phase pumps were stopped.

(23) All fluids were removed from the pumping chambers.

(24) The FCC and Pixelink software were shut down, and the pumps were turned off.

(25) The valve for the helium gas tank was closed, the pressure that was trapped in the tubing was released by opening the air filter to the air pressure, and then the valve was closed for the two-stage pressure regulator.

Troubleshooting tip: During the polymer droplet collection, there may be unforeseen pressure changes that can lead to droplet formation with varied sizes and subsequent polydispersity of the particles. In such a case, the droplet collection vial should be quickly replaced with the waste vial, and the system should continue to flow until the flow rates become stable again. Then, the droplet collection can be resumed. However, pressure fluctuation with a dramatic and sudden pressure change requires immediate cessation of the fluid flow. This usually occurs if there is a clogging issue in the droplet generator. In this case, pressure pumps that have been working under the flow control mode

https://doi.org/10.1021/acsbiomaterials.2c00066
ACS Biomater. Sci. Eng. 2022, 8, 2864−2877

Table 3. Commercially Available Droplet Generators and Their Specifications

material	configuration	droplet diameter	emulsion type	surface coating	provider
PDMS	T-junction flow focusing	15−1500 μm	O/W	hydrophilic	Dropletex[a]
			W/O	hydrophobic	Dropletex
	flow focusing	30−100 μm	W/O	none	Elveflow
	T-junction flow focusing	30−300 μm	W/O	none	Darwin Microfluidics
glass	T-junction flow focusing	2−150 μm	O/W	hydrophilic	Dolomite
			W/O W/O/W[b]	hydrophobic fluorophilic	Dolomite
	flow focusing	9−140 μm	O/W	hydrophilic	Micronit[a]
			W/O W/O/W[c]	hydrophobic	Micronit
	flow focusing	40−250 μm	O/W	hydrophilic	Darwin Microfluidics
PC	T-junction flow focusing	10−100 μm	O/W W/O	none	microfluidic ChipShop[a]
COC	T-junction flow focusing	10−100 μm	O/W	none	microfluidic ChipShop
			W/O		microfluidic ChipShop
	flow focusing	20−100 μm	O/W W/O	none	On-Chip Technologies
PMMA	Y-junction flow focusing	30−80 μm	O/W	hydrophilic	Cellix
			W/O	hydrophobic	Cellix
resin	coflow focusing	40−130 μm	O/W W/O	none	Fluigent

[a]Provider offers custom-designed device production for a given device configuration. [b]Two droplet generators are connected in series. [c]Single device.

should be immediately switched to the pressure control mode. The droplet collection vial should be replaced with the waste vial. All in-line valves should be turned off, and all the pumps should be stopped.

Cleaning the Droplet Generator. It is recommended to clean the droplet generator with compatible solvents. Notably, it would be practical to clean the device with the solvents that are used for the droplet generation. In this study, the continuous and dispersed phases were prepared by using filtered water and DCM, and therefore the droplet generator was initially cleaned with these solvents. Briefly, a 20 mL vial of filtered Milli-Q water was placed in the chamber of the continuous phase pump, and the in-line valves V2, V3, and V4 were kept closed. Then, the system was flushed with water for 3−5 min at 3000 mbar, the highest pressure level at which the droplet generator can work. Similarly, the in-line valves V1 and V3 were kept closed before flushing the system with DCM for 3−5 min at 3000 mbar. Flushing the system with water and DCM helped to remove polymer and surfactant residues (PLGA and PVA in this case) in the droplet generator and the connecting tubing. To ensure the removal of any undesired solids that could not be removed completely by these solvents due to their solvent resistance, different solvents can be flushed through the system. Because the glass droplet generator used herein was compatible with various solvents, including organic solvents, strong acid (1 M HCl), and base (1 M NaOH), it was quite straightforward to find the best cleaning solvent. To prepare the device for flushing with a strong acid or base solution, one of the inlets was used to introduce the cleaning acid/base solution as the other inlets were disassembled from the connection points (in-line valves V1 and V4), so that the cleaning solution left the device from these open ends. Then, the device was flushed with water to remove the acid/base residue. Finally, the device was completely dried to be prepared for the next use.

Solidification of Polymer Droplets for Particle Formation and Purification. The solidification of polymer droplets for particle formation and purification followed these steps:

(1) Each droplet collection vial was kept stirring for 3 h in a fume hood for complete DCM evaporation and solidification of droplets for particle formation.

(2) The particle suspension solutions were combined in a 50 mL falcon tube and centrifuged at 100 × *g* for 5 min.

(3) The supernatant was removed, 30 mL of Milli-Q water was added, and the particles were resuspended by pipetting up and down and then vortexing at the maximum speed for 10 s.

Troubleshooting tip: The purification step aims to remove surfactant (in this case, PVA) from the aqueous collection solution before the freeze-drying process. Resuspension of particles in PVA-free water in each washing step may cause particle aggregation. To eliminate this problem, 1−2 mL of water is added to the particles once the supernatant is removed and then gently mixed while pipetting up and down. When all of the particles are homogeneously suspended, water is added to a final volume of 30 mL. Alternatively, particles are centrifuged at a slower speed, such as 50−75 × *g*.

(4) The washing process was repeated three times.

(5) When the supernatant was removed for the final washing step, the particles were resuspended in 1 mL of Milli-Q water, transferred in a glass vial, and flash frozen in liquid nitrogen. The glass vial was weighed before transferring the particle suspension so the particle yield can be quantified.

(6) The vial was placed in a lyophilizer overnight.

(7) The vial was weighed to calculate the total weight of dry particles, and the particles were stored at −20 °C.

Preparation of PLGA Microparticles via Traditional Batch Method. PLGA microparticles were fabricated using a single emulsion−evaporation technique. Briefly, 200 mg of PLGA was dissolved in 4 mL of DCM. This solution was homogenized with 60 mL of 2% PVA solution at 3 000 rpm mixing speed for 1 min. The emulsion was then mixed with 80 mL of 1% PVA solution. The final emulsion solution was stirred for 3 h to remove DCM and to form solid PLGA microparticles. The microparticle suspension was washed 5 times with deionized water and lyophilized for 48 h.

Step 4: Characterization of Particles. *Particle Size and Morphology.* To characterize PLGA microparticles in size and morphology, scanning electron microscopy (SEM; Zeiss Sigma 500VP microscope) was used to capture images of the samples. PLGA microparticles are usually affected by the high-energy electron beam that induces heat-associated particle degradation during the imaging process. One way to overcome the particle degradation issue is to reduce the beam energy. Therefore, the SEM images were taken at a low beam energy level (1 keV). Then, MATLAB was employed to analyze the microparticle images to determine the mean size and size distribution of PLGA microparticles. The MATLAB code is designed on the Circular Hough Transform based algorithm for identifying circles in images and reporting their radius and center location.[55−57] The MATLAB code was set to detect an average of 100 circles in images for each sample, report back their radius and center location, and then draw and overlay circles on the microparticles using the built-in MATLAB function *viscircles*. For each sample, 6−9 SEM images were used.

Drug Encapsulation Efficiency. Drug (rapamycin)-containing polymer (PLGA) particles and drug-free controls (n = 4, 5 mg) were dissolved in 500 μL of acetonitrile, and the mixture was vortexed for 10 min. One hundred μL of the mixture was used to measure absorbance values at 278 nm, and then the amount of rapamycin was calculated from these absorption values using a standard curve. The drug

https://doi.org/10.1021/acsbiomaterials.2c00066
ACS Biomater. Sci. Eng. 2022, 8, 2864−2877

encapsulation efficiency was calculated from the following equation: encapsulation efficiency = (actual drug amount/theoretical drug amount) × 100.

■ ANTICIPATED RESULTS

We screened the commercial microfluidic supply landscape to outline the commercialized droplet generators, and the results of the device specifications are in Table 3. According to this inventory, we identified different droplet generators that could produce droplets with diameters ranging from 10 to 1500 μm. In addition, these devices offered different nozzle configurations such as T-junction, flow focusing, coflow focusing, and Y-junction with the capacity to produce single or double emulsions. In terms of the device material type, several different options were identified. In general, the availability of these different materials broadened the choice of immiscible solvent combinations with which the droplet generator was compatible. Further, droplet generators with a hydrophobic surface coating were also commercially available. Such coatings on microchannel surfaces enhance the surface wettability with the continuous phase; thus, droplet stability is maintained during the droplet generation and collection processes. Overall, this inventory allowed us to identify the optimum droplet generator capable of encapsulating a hydrophobic drug, rapamycin, in a hydrophobic polymeric drug carrier, PLGA. The PLGA droplets were intended to be generated in the form of O/W emulsions with DCM and water as the immiscible phases. On the basis of the optimum solvent compatibility, especially for DCM, we selected a glass droplet generator with a hydrophilic microchannel surface. Additionally, this droplet generator had a flow-focusing nozzle configuration with a 100 μm wide and 105 μm long elliptical geometry that could produce PLGA microparticles with a target particle size of 9−20 μm.

Once the other components of the microfluidic system were determined, the representative microfluidic setup was used to demonstrate its flexibility to generate polymer droplets with various sizes. A number of process parameters, such as flow rates of continuous and dispersed phases, PLGA concentration in the dispersed phase, and surfactant type and concentration in the continuous phase, affect the size of the droplets and subsequently the microparticles. In this report, we focused on the effects of flow rates and concentration of polymer (PLGA) on the droplet and microparticle size. The effects of surfactant type and concentration were not studied in this work given that the continuous phase was chosen from the proprietary commercial aqueous formulation.

Prior to investigating the effect of process parameters on the polymer droplet size using the aforementioned microfluidic setup, the formation of dripping and jetting flow regimes at each flow condition were initially identified for the dispersed phase that was 2% PLGA in DCM solution. In general, the dripping regime occurred at the flow conditions when monodisperse droplets were formed, whereas the jetting flow regime was observed in the form of a liquid thread of the dispersed phase within the continuous phase, resulting in the generation of droplets with nonuniform size distribution. For this study, the flow rate of the continuous phase was gradually increased starting from 30 μL/min, which is the minimum continuous flow rate that the flow sensor could measure reliably. Then, the maximum continuous phase flow rate at which the dripping regime switched to the jetting regime was recorded by capturing a short video. Video SI1 and Video SI2 represent two example videos for dripping and jetting flow regimes with continuous-phase flow rates of 50 and 100 μL/min, respectively, and a dispersed phase flow rate of 8 μL/min. Similarly, dripping and jetting flow regimes were identified for other dispersed-phase flow rates, ranging between 1 and 13 μL/min, that were within the limits for the flow sensor (1−50 μL/min). As a result, the highest flow rates for the dispersed and continuous phases at the dripping regime were determined to be 10 and 140 μL/min, respectively. Table 4 summarizes possible working flow conditions where the dripping regime with monodisperse droplet production was observed as well as the flow conditions for heterogeneous droplet production where the jetting forms.

Table 4. Summary of the Flow Rates of Dispersed and Continuous Phases at Which Dripping and Jetting Flow Regimes for 2% PLGA Solution Were Observed[a]

Continuous phase flow rate (μL/min) \ Dispersed phase flow rate (μL/min)	1	2	3	4	5	6	7	8	9	10	11	12	13
30	D	D	D	D	D	D	D	D	D	D	J	J	J
40	D	D	D	D	D	D	D	D	D	J	J	J	J
50	D	D	D	D	D	D	D	D	D	J	J	J	J
60	D	D	D	D	D	D	D	D	D	J	J	J	J
70	D	D	D	D	D	D	D	D	D	J	J	J	J
80	D	D	D	D	D	D	D	D	J	J	J	J	J
90	D	D	D	D	D	D	D	J	J	J	J	J	J
100	D	D	D	D	D	D	J	J	J	J	J	J	J
110	D	D	D	D	D	D	J	J	J	J	J	J	J
120	D	D	D	D	D	J	J	J	J	J	J	J	J
130	D	D	D	D	J	J	J	J	J	J	J	J	J
140	J	J	D	D	J	J	J	J	J	J	J	J	J
150	J	J	J	J	J	J	J	J	J	J	J	J	J

[a]D and J represent dripping and jetting flow regimes, respectively.

Next, droplet size as a function of flow rates of the immiscible and dispersed phases was determined for a 2% PLGA solution in DCM (Figure 4). For a given continuous phase flow rate, a direct correlation between the PLGA droplet size and the dispersed phase flow rate was observed. For example, PLGA droplets with size (mean ± SD) ranging from 71.7 ± 2.3 to 81.9 ± 0.5 μm were formed at the continuous flow rate of 30 μL/min when the dispersed phase flow rate was increased from 1 to 9 μL/min, respectively. In contrast, the droplet size was inversely

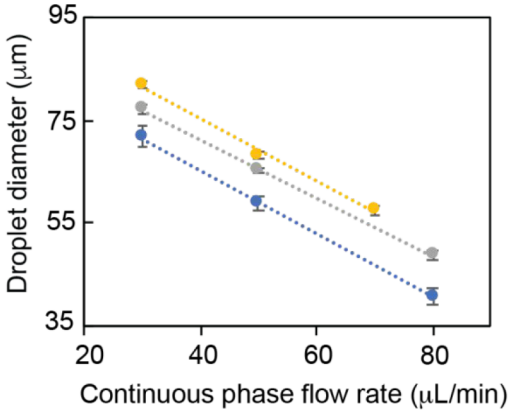

Figure 4. PLGA droplet size as a function of the flow rates of continuous and dispersed phases. Droplet size was measured at constant flow rates for the dispersed phase (1 (blue), 6 (gray), and 9 μL/min (yellow)) while altering the flow rate of the continuous phase. Eight data points for each flow condition were used to determine the droplet size, and error bars were calculated based on the standard deviations of these measurements.

https://doi.org/10.1021/acsbiomaterials.2c00066
ACS Biomater. Sci. Eng. 2022, 8, 2864−2877

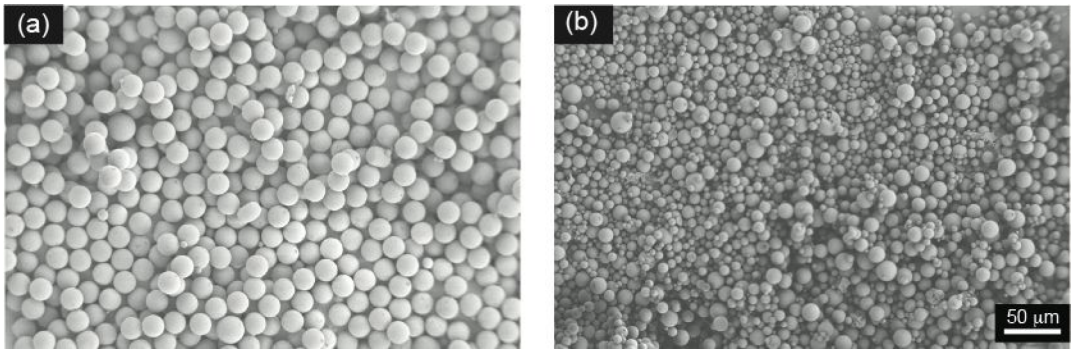

Figure 5. Representative scanning electron micrograph of PLGA microparticles that are prepared by (a) microfluidic and (b) traditional batch methods. The micrographs demonstrate the size distribution with surface morphology. Droplet generation parameters: 2% PLGA solution with dispersed phase flow rate of 4 μL/min and continuous phase flow rate of 30 μL/min. Representative scanning electron micrographs were taken under 250× magnification.

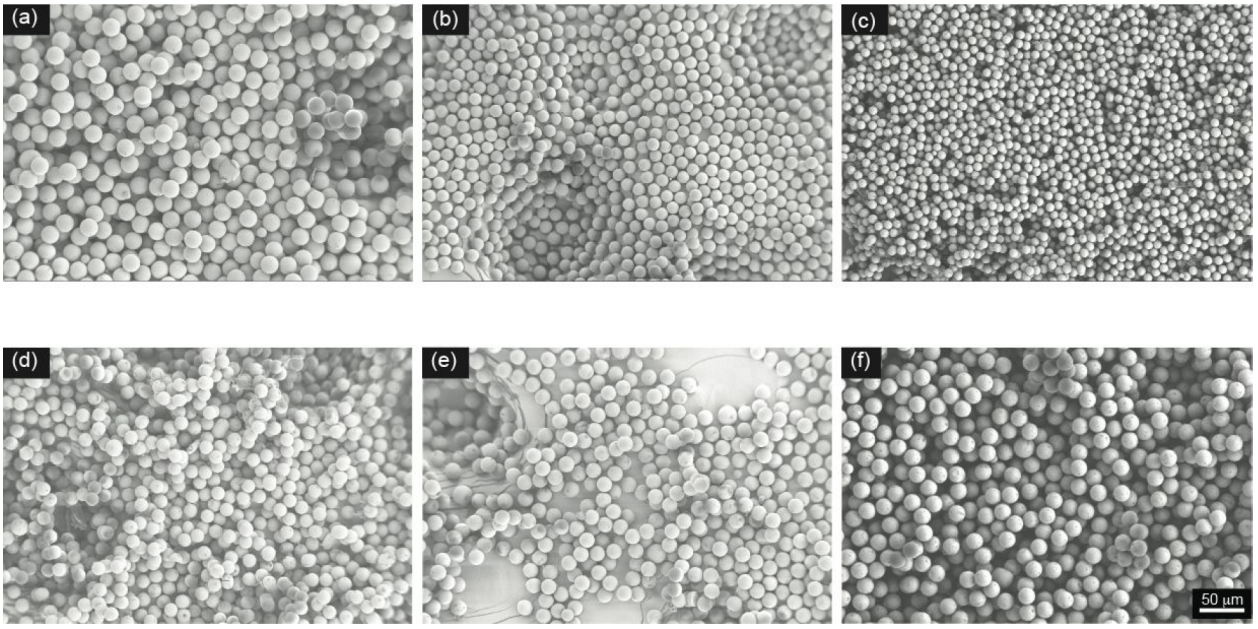

Figure 6. PLGA microparticle size changes as a function of flow conditions. Scanning electron micrographs with droplet generation parameters of 2% PLGA solution with a flow rate of 4 μL/min and continuous phase flow rates of (a) 30, (b) 80, and (c) 110 μL/min. Scanning electron micrographs with droplet generation parameters of a continuous phase flow rate of 50 μL/min and 2% PLGA solution with a flow rate of (d) 1, (e) 4, and (f) 9 μL/min. Representative scanning electron micrographs were taken under 250× magnification.

correlated with the continuous phase flow rate for a given dispersed phase flow condition. Accordingly, PLGA droplet sizes decreased from 77.1 ± 0.8 to 48.7 ± 1 μm as the continuous phase flow rate was increased from 30 to 80 μL/min when the dispersed phase flow rate was set to 6 μL/min. Both droplet size and droplet generation rate or frequency were affected by the flow rates of the dispersed and continuous phases (Figure SI1). In general, higher flow rates of the dispersed phase resulted in faster production of the PLGA droplets. Overall, PLGA droplets with diameters ranging from 40.8 ± 1.7 to 85.3 ± 0.8 μm within the dripping flow regime were produced by tuning the flow rates of dispersed and continuous phases.

The droplet production was followed by a postfabrication process that converted the collected droplets to solid PLGA microparticles. In this process, DCM was evaporated by stirring the PLGA droplet suspension solution under a constant, mild mixing condition. Notably, it was critical to maintain the droplet stability and to minimize random fusion of the polymer droplets during this process. Therefore, an aqueous solution of emulsifier (PVA) was used as the droplet-collection solution. Otherwise, the postfabrication process would result in PLGA microparticles with polydisperse size distribution due to coalescence of the droplets. As DCM gradually evaporated from the PLGA droplets under atmospheric pressure via a diffusion-controlled mass transfer, the droplets underwent a reduction in their size, and finally solid microparticles were formed.[58−60] Monodisperse PLGA microparticles with a diameter (mean ± SD) of 19.3 ± 0.6 μm (coefficient of variation (CV) = 3.1%) were obtained from PLGA droplets that were generated from a 2% PLGA solution with a flow rate of 4 μL/min, while the flow rate of continuous phase was set to 30 μL/min. Additionally, the smooth surface morphology of PLGA microparticles was confirmed by the SEM imaging (Figure 5a). However, PLGA microparticles that were prepared by the traditional batch method demonstrated a polydisperse size distribution with a diameter of 8.6 ± 3.3 μm (CV = 38.9%) (Figure 5b).

Further, PLGA droplets with various sizes were processed through the solvent (DCM)-evaporation step to investigate the

https://doi.org/10.1021/acsbiomaterials.2c00066
ACS Biomater. Sci. Eng. 2022, 8, 2864−2877

relationship between the size of the PLGA microparticles and the flow rate of the immiscible solvents (Figure 6). In this part of the work, PLGA droplets were prepared using 2% PLGA solution in DCM. Particle-size characterization revealed a reduction in the particle size with increasing flow rate of the continuous phase at a constant flow of the dispersed phase. Moreover, larger PLGA particles were obtained when the flow rate of the dispersed phase was increased while keeping the flow rate of the continuous phase constant. Specifically, for a flow rate of the dispersed phase of 4 μL/min, PLGA microparticle diameters decreased from 19.3 ± 0.6 to 9.1 ± 0.4 μm as the continuous phase flow rate was increased from 30 to 110 μL/min (Figure 6a–c). If the continuous phase flow rate was set at 50 μL/min and the dispersed phase flow rate increased from 1 to 9 μL/min, the size of the PLGA microparticles increased from 14.5 ± 0.5 to 17.9 ± 0.8 μm (Figure 6d–f). These results were in good agreement with the change in the PLGA droplet size that is shown in Figure 4. On the basis of these size measurements, we observed a reduction in the droplet diameter of 70–75% during PLGA microparticle solidification, corresponding to a reduction in droplet volume of 97.3–98.4%. Furthermore, the correlation between PLGA microparticle size and droplet size was investigated for the samples that were prepared at the set continuous phase flow rate of 50 μL/min and dispersed phase flow rates of 1, 4, and 9 μL/min (Figure 7). The linear regression equation for this correlation ($y = 0.2587x$) was very close to the theoretical equation ($y = 0.2487x$), where y represented the microparticle diameter and x was the droplet diameter. The theoretical equation can be simplified as the following: microparticle diameter (y) = [(PLGA concentration/PLGA density)$^{1/3}$] × droplet diameter (x), where the PLGA concentration is 0.02 (2% (w/v) solution) and the PLGA density is 1.3 g/cm^3.

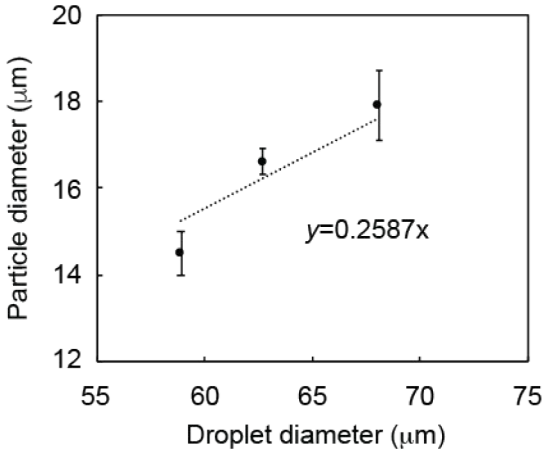

Figure 7. Correlation between PLGA microparticle and droplet sizes. Droplet generation parameters: 2% PLGA solution with flow rates of 1, 4, and 9 μL/min and a continuous phase flow rate of 50 μL/min.

To study how polymer concentration affects particle size, droplets using two different polymer concentrations, 2% (w/v) and 5% (w/v), in the dispersed phase were produced using dispersed and continuous phases with flow rates of 4 and 80 μL/min, respectively. Then, the size of the solidified polymer microparticles was measured. As expected, there was an increase in particle size with increasing PLGA content in the dispersed phase. Specifically, the microparticles with mean diameters of 14.7 ± 0.5 and 16.5 ± 0.5 μm were obtained with 2% (w/v) and 5% (w/v) PLGA concentrations, respectively. However, there was no change in the polydispersity (CV < 5%), and monodisperse particles were confirmed by the SEM images (Figure 8).

To further demonstrate the capacity of the developed microfluidic system, PLGA-based microparticles encapsulating a hydrophobic drug, rapamycin, were produced using the dispersed phase prepared by mixing rapamycin with 5% (w/v) PLGA solution in DCM. Rapamycin was loaded at a drug/PLGA ratio of 5 μg drug/mg PLGA. The drug encapsulation efficiency in the PLGA microparticles was determined to be 89.4 ± 1.6%, thereby indicating a high and reproducible drug encapsulation into PLGA microparticles using the microfluidic system.

SUMMARY

This study presented a framework to facilitate the design, construction, and operation of a microfluidic setup using commercially available components for the production of highly uniform, drug-loaded biodegradable particles. Practical guidelines for the rational selection of a microfluidic device and other accessory equipment were provided. For the selection of a droplet generator, a determination of the optimal immiscible solvents for the target emulsion was the key to identifying a compatible droplet generator material type. Additionally, configurational aspects of the droplet generator, including the size and geometry of the microchannels, were other important parameters that shaped the decision-making process. The

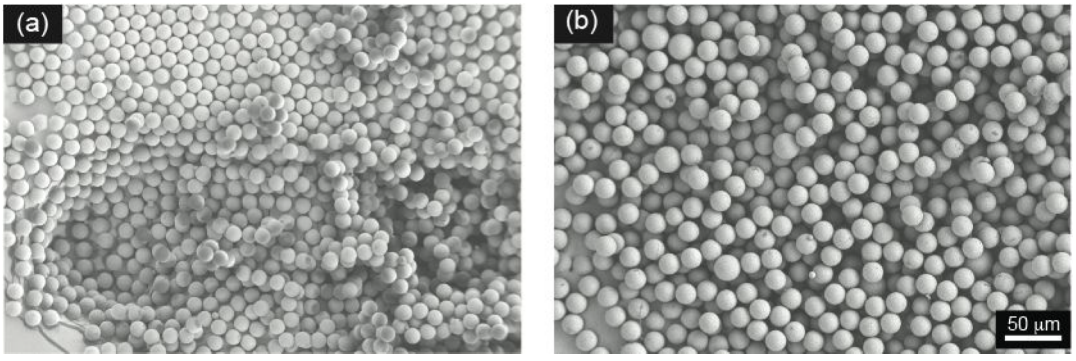

Figure 8. PLGA microparticle size tuned by changing the PLGA concentration in the dispersed phase. Microparticles were prepared with (a) 2% (w/v) PLGA and (b) 5% (w/v) PLGA solutions using dispersed and continuous phases with flow rates of 4 and 80 μL/min, respectively. Representative scanning electron micrographs were taken under 250× magnification.

https://doi.org/10.1021/acsbiomaterials.2c00066
ACS Biomater. Sci. Eng. 2022, 8, 2864–2877

compatibility of the droplet generator with other system components, such as fluid control systems and connecting tools, was also discussed.

A representative microfluidic setup was devised by implementing the presented framework to encapsulate a hydrophobic drug, rapamycin, in a hydrophobic polymer drug carrier, PLGA, via O/W emulsion. The operational aspects of this microfluidic setup, especially in the context of altering the size of the PLGA droplets and subsequently the resulting microparticles, were described. Finally, the PLGA microparticles were shown to have a high and reproducible drug encapsulation efficiency. Together, the presented guidelines may enable widespread adoption of droplet microfluidics to engineer drug-loaded biodegradable microparticles.

■ ASSOCIATED CONTENT

Supporting Information

The Supporting Information is available free of charge at https://pubs.acs.org/doi/10.1021/acsbiomaterials.2c00066.

PLGA droplet size and frequency change as the flow rate changes (PDF)

Droplets of 2% PLGA solution in the dripping-flow regime (MP4)

Droplets of 2% PLGA solution in the jetting-flow regime (MP4)

■ AUTHOR INFORMATION

Corresponding Author

Steven R. Little − *Department of Chemical Engineering, University of Pittsburgh, Pittsburgh, Pennsylvania 15261, United States; Department of Bioengineering and Department of Pharmaceutical Sciences, University of Pittsburgh, Pittsburgh, Pennsylvania 15261, United States; The McGowan Institute for Regenerative Medicine, University of Pittsburgh, Pittsburgh, Pennsylvania 15219, United States; Department of Immunology and Department of Ophthalmology, University of Pittsburgh, Pittsburgh, Pennsylvania 15213, United States;* orcid.org/0000-0002-7000-3931; Email: srlittle@pitt.edu

Authors

Nihan Yonet-Tanyeri − *Department of Chemical Engineering, University of Pittsburgh, Pittsburgh, Pennsylvania 15261, United States*

Maher Amer − *Department of Dermatology, University of Pittsburgh School of Medicine, Pittsburgh, Pennsylvania 15213, United States*

Stephen C. Balmert − *Department of Dermatology, University of Pittsburgh School of Medicine, Pittsburgh, Pennsylvania 15213, United States*

Emrullah Korkmaz − *Department of Dermatology, University of Pittsburgh School of Medicine, Pittsburgh, Pennsylvania 15213, United States; Department of Bioengineering, University of Pittsburgh, Pittsburgh, Pennsylvania 15261, United States*

Louis D. Falo, Jr. − *Department of Dermatology, University of Pittsburgh School of Medicine, Pittsburgh, Pennsylvania 15213, United States; Department of Bioengineering, University of Pittsburgh, Pittsburgh, Pennsylvania 15261, United States; Clinical and Translational Science Institute, University of Pittsburgh, Pittsburgh, Pennsylvania 15213, United States; The McGowan Institute for Regenerative Medicine, University of Pittsburgh, Pittsburgh, Pennsylvania 15219, United States*

Complete contact information is available at: https://pubs.acs.org/10.1021/acsbiomaterials.2c00066

Author Contributions

N.Y.-T. designed the experiments, and N.Y.-T. and M.A. performed the experiments. All authors reviewed and edited the paper. All authors approved the final version of the manuscript.

Notes

The authors declare no competing financial interest.

■ ACKNOWLEDGMENTS

This work was supported in part by the NIH Grant R01-AR074285 and the Commonwealth of Pennsylvania's Department of Community and Economic Development (DCED).

■ REFERENCES

(1) Choi, A.; Seo, K. D.; Kim, D. W.; Kim, B. C.; Kim, D. S. Recent advances in engineering microparticles and their nascent utilization in biomedical delivery and diagnostic applications. *Lab Chip* **2017**, *17* (4), 591−613.

(2) Feng, Q.; Sun, J.; Jiang, X. Microfluidics-mediated assembly of functional nanoparticles for cancer-related pharmaceutical applications. *Nanoscale* **2016**, *8* (25), 12430−43.

(3) Pinto Reis, C.; Neufeld, R. J.; Ribeiro, A. J.; Veiga, F. Nanoencapsulation I. Methods for preparation of drug-loaded polymeric nanoparticles. *Nanomedicine* **2006**, *2* (1), 8−21.

(4) Wang, W.; Zhang, M. J.; Chu, L. Y. Functional polymeric microparticles engineered from controllable microfluidic emulsions. *Acc. Chem. Res.* **2014**, *47* (2), 373−84.

(5) Whitesides, G. M. The origins and the future of microfluidics. *Nature* **2006**, *442* (7101), 368−73.

(6) Liu, D.; Zhang, H.; Fontana, F.; Hirvonen, J. T.; Santos, H. A. Microfluidic-assisted fabrication of carriers for controlled drug delivery. *Lab Chip* **2017**, *17* (11), 1856−1883.

(7) Li, W.; Zhang, L.; Ge, X.; Xu, B.; Zhang, W.; Qu, L.; Choi, C.-H.; Xu, J.; Zhang, A.; Lee, H.; Weitz, D. A. Microfluidic fabrication of microparticles for biomedical applications. *Chem. Soc. Rev.* **2018**, *47* (15), 5646−5683.

(8) Yasuda, S.; Hayakawa, M.; Onoe, H.; Takinoue, M. Twisting microfluidics in a planetary centrifuge. *Soft Matter* **2017**, *13* (11), 2141−2147.

(9) Cheng, Y.; Zhang, X.; Cao, Y.; Tian, C.; Li, Y.; Wang, M.; Zhao, Y.; Zhao, G. Centrifugal microfluidics for ultra-rapid fabrication of versatile hydrogel microcarriers. *Appl. Mater. Today* **2018**, *13*, 116−125.

(10) Ahmed, N.; Sukovich, D.; Abate, A. R. Operation of Droplet-Microfluidic Devices with a Lab Centrifuge. *Micromachines (Basel)* **2016**, *7* (9), 161.

(11) Zhao, G.; Liu, X.; Zhu, K.; He, X. Hydrogel Encapsulation Facilitates Rapid-Cooling Cryopreservation of Stem Cell-Laden Core-Shell Microcapsules as Cell-Biomaterial Constructs. *Adv. Healthcare Mater.* **2017**, *6* (23), 1700988.

(12) Riahi, R.; Tamayol, A.; Shaegh, S. A. M.; Ghaemmaghami, A.; Dokmeci, M. R.; Khademhosseini, A. Microfluidics for Advanced Drug Delivery Systems. *Curr. Opin Chem. Eng.* **2015**, *7*, 101−112.

(13) Sanjay, S. T.; Zhou, W.; Dou, M.; Tavakoli, H.; Ma, L.; Xu, F.; Li, X. Recent advances of controlled drug delivery using microfluidic platforms. *Adv. Drug Deliv Rev.* **2018**, *128*, 3−28.

(14) Jeong, W. J.; Kim, J. Y.; Choo, J.; Lee, E. K.; Han, C. S.; Beebe, D. J.; Seong, G. H.; Lee, S. H. Continuous Fabrication of Biocatalyst Immobilized Microparticles Using Photopolymerization and Immiscible Liquids in Microfluidic Systems. *Langmuir* **2005**, *21* (9), 3738−3741.

(15) Zhao, Y.; Shum, H. C.; Adams, L. L. A.; Sun, B.; Holtze, C.; Gu, Z.; Weitz, D. A. Enhanced Encapsulation of Actives in Self-Sealing Microcapsules by Precipitation in Capsule Shells. *Langmuir* **2011**, *27* (23), 13988−13991.
(16) Sugiura, S.; Oda, T.; Izumida, Y.; Aoyagi, Y.; Satake, M.; Ochiai, A.; Ohkohchi, N.; Nakajima, M. Size control of calcium alginate beads containing living cells using micro-nozzle array. *Biomaterials* **2005**, *26* (16), 3327−3331.
(17) Xu, Q.; Hashimoto, M.; Dang, T. T.; Hoare, T.; Kohane, D. S.; Whitesides, G. M.; Langer, R.; Anderson, D. G. Preparation of Monodisperse Biodegradable Polymer Microparticles Using a Microfluidic Flow-Focusing Device for Controlled Drug Delivery. *Small* **2009**, *5* (13), 1575−1581.
(18) Seo, M.; Paquet, C.; Nie, Z.; Xu, S.; Kumacheva, E. Microfluidic consecutive flow-focusing droplet generators. *Soft Matter* **2007**, *3* (8), 986−992.
(19) Volpatti, L. R.; Yetisen, A. K. Commercialization of microfluidic devices. *Trends Biotechnol.* **2014**, *32* (7), 347−350.
(20) Li, L.; Schwendeman, S. P. Mapping neutral microclimate pH in PLGA microspheres. *J. Controlled Release* **2005**, *101* (1−3), 163−73.
(21) Jhunjhunwala, S.; Balmert, S. C.; Raimondi, G.; Dons, E.; Nichols, E. E.; Thomson, A. W.; Little, S. R. Controlled release formulations of IL-2, TGF-β1 and rapamycin for the induction of regulatory T cells. *Journal of controlled release: official journal of the Controlled Release Society* **2012**, *159* (1), 78−84.
(22) Washington, M. A.; Balmert, S. C.; Fedorchak, M. V.; Little, S. R.; Watkins, S. C.; Meyer, T. Y. Monomer sequence in PLGA microparticles: Effects on acidic microclimates and in vivo inflammatory response. *Acta Biomater* **2018**, *65*, 259−271.
(23) Makadia, H. K.; Siegel, S. J. Poly Lactic-co-Glycolic Acid (PLGA) as Biodegradable Controlled Drug Delivery Carrier. *Polymers (Basel)* **2011**, *3* (3), 1377−1397.
(24) Rothstein, S. N.; Federspiel, W. J.; Little, S. R. A unified mathematical model for the prediction of controlled release from surface and bulk eroding polymer matrices. *Biomaterials* **2009**, *30* (8), 1657−1664.
(25) Rothstein, S. N.; Kay, J. E.; Schopfer, F. J.; Freeman, B. A.; Little, S. R. A Retrospective Mathematical Analysis of Controlled Release Design and Experimentation. *Mol. Pharmaceutics* **2012**, *9* (11), 3003−3011.
(26) Kim, Y.; Park, E. J.; Kim, T. W.; Na, D. H. Recent Progress in Drug Release Testing Methods of Biopolymeric Particulate System. *Pharmaceutics* **2021**, *13* (8), 1313.
(27) Larsen, C.; Larsen, S. W.; Jensen, H.; Yaghmur, A.; Østergaard, J. Role of in vitro release models in formulation development and quality control of parenteral depots. *Expert Opinion on Drug Delivery* **2009**, *6* (12), 1283−1295.
(28) Baimark, Y.; Srisuwan, Y. Preparation of alginate microspheres by water-in-oil emulsion method for drug delivery: Effect of Ca2+ post-cross-linking. *Advanced Powder Technology* **2014**, *25* (5), 1541−1546.
(29) Li, Z.; Kuang, H.; Yang, J.; Hu, J.; Ding, B.; Sun, W.; Luo, Y. Improving emulsion stability based on ovalbumin-carboxymethyl cellulose complexes with thermal treatment near ovalbumin isoelectric point. *Sci. Rep.* **2020**, *10* (1), 3456.
(30) Zamora-Mora, V.; Velasco, D.; Hernández, R.; Mijangos, C.; Kumacheva, E. Chitosan/agarose hydrogels: Cooperative properties and microfluidic preparation. *Carbohydr. Polym.* **2014**, *111*, 348−355.
(31) Peng, H.; Xiong, H.; Li, J.; Xie, M.; Liu, Y.; Bai, C.; Chen, L. Vanillin cross-linked chitosan microspheres for controlled release of resveratrol. *Food Chem.* **2010**, *121* (1), 23−28.
(32) Jay, S. M.; Saltzman, W. M. Controlled delivery of VEGF via modulation of alginate microparticle ionic crosslinking. *J. Controlled Release* **2009**, *134* (1), 26−34.
(33) Kirubanandan, S. Ciprofloxacin-Loaded Gelatin Microspheres Impregnated Collagen Scaffold for Augmentation of Infected Soft Tissue. *Asian J. Pharm.* **2017**, *11* (02); DOI: 10.22377/ajp.v11i02.1158.
(34) Karataş, A.; Sonakin, O.; Kiliçarslan, M.; Baykara, T. Poly (epsilon-caprolactone) microparticles containing Levobunolol HCl prepared by a multiple emulsion (W/O/W) solvent evaporation technique: effects of some formulation parameters on microparticle characteristics. *J. Microencapsul* **2009**, *26* (1), 63−74.
(35) Tsirigotis-Maniecka, M. Alginate-, Carboxymethyl Cellulose-, and κ-Carrageenan-Based Microparticles as Storage Vehicles for Cranberry Extract. *Molecules* **2020**, *25* (17), 3998.
(36) Icart, L. P.; Souza, F. G. d.; Lima, L. M. T. R. Sustained release and pharmacologic evaluation of human glucagon-like peptide-1 and liraglutide from polymeric microparticles. *J. Microencapsulation* **2019**, *36* (8), 747−758.
(37) Damiati, S. A.; Damiati, S. Microfluidic Synthesis of Indomethacin-Loaded PLGA Microparticles Optimized by Machine Learning. *Front Mol. Biosci* **2021**, *8*, 677547−677547.
(38) Wischke, C.; Schwendeman, S. P. Principles of encapsulating hydrophobic drugs in PLA/PLGA microparticles. *Int. J. Pharm.* **2008**, *364* (2), 298−327.
(39) Busatto, C. A.; Labie, H.; Lapeyre, V.; Auzely-Velty, R.; Perro, A.; Casis, N.; Luna, J.; Estenoz, D. A.; Ravaine, V. Oil-in-microgel strategy for enzymatic-triggered release of hydrophobic drugs. *J. Colloid Interface Sci.* **2017**, *493*, 356−364.
(40) Schroën, K.; de Ruiter, J.; Berton-Carabin, C. The Importance of Interfacial Tension in Emulsification: Connecting Scaling Relations Used in Large Scale Preparation with Microfluidic Measurement Methods. *ChemEngineering* **2020**, *4* (4), 63.
(41) Peng, L.; Yang, M.; Guo, S.-s.; Liu, W.; Zhao, X.-z. The effect of interfacial tension on droplet formation in flow-focusing microfluidic device. *Biomed. Microdevices* **2011**, *13* (3), 559−564.
(42) Amoyav, B.; Benny, O. Controlled and tunable polymer particles' production using a single microfluidic device. *Applied Nanoscience* **2018**, *8* (4), 905−914.
(43) Henshaw, C. A.; Dundas, A. A.; Cuzzucoli Crucitti, V.; Alexander, M. R.; Wildman, R.; Rose, F. R. A. J.; Irvine, D. J.; Williams, P. M. Droplet Microfluidic Optimisation Using Micropipette Characterisation of Bio-Instructive Polymeric Surfactants. *Molecules* **2021**, *26* (11), 3302.
(44) Ho, T. M.; Razzaghi, A.; Ramachandran, A.; Mikkonen, K. S. Emulsion characterization via microfluidic devices: A review on interfacial tension and stability to coalescence. *Adv. Colloid Interface Sci.* **2022**, *299*, 102541.
(45) Baret, J. C. Surfactants in droplet-based microfluidics. *Lab Chip* **2012**, *12* (3), 422−33.
(46) Microfluidic Droplet Generators. https://darwin-microfluidics.com/collections/microfluidic-droplet-generators (accessed Jan 2022).
(47) Lee, J. N.; Park, C.; Whitesides, G. M. Solvent Compatibility of Poly(dimethylsiloxane)-Based Microfluidic Devices. *Anal. Chem.* **2003**, *75* (23), 6544−6554.
(48) How to select the right microfluidic pump? https://www.fluigent.com/resources/microfluidic-expertise/advantages-of-pressure-based-microfluidic/system-comparison-for-microfluidic-applications/ (accessed Jan 2022).
(49) Mavrogiannis, N.; Ibo, M.; Fu, X.; Crivellari, F.; Gagnon, Z. Microfluidics made easy: A robust low-cost constant pressure flow controller for engineers and cell biologists. *Biomicrofluidics* **2016**, *10* (3), 034107−034107.
(50) Zeng, W.; Li, S.; Wang, Z. Characterization of syringe-pump-driven versus pressure-driven microfluidic flows. In *Proceedings of 2015 International Conference on Fluid Power and Mechatronics (FPM)*, August 5−7, 2015; IEEE: 2015; pp 711−715; DOI: 10.1109/FPM.2015.7337207.
(51) Kalantarifard, A.; Alizadeh-Haghighi, E.; Saateh, A.; Elbuken, C. Theoretical and experimental limits of monodisperse droplet generation. *Chem. Eng. Sci.* **2021**, *229*, 116093.
(52) The Basics of Microfuidic Tubings and Sleeves. https://www.elveflow.com/microfluidic-reviews/general-microfluidics/the-basics-of-microfluidic-tubing-sleeves/ (accessed Jan 2022).
(53) High-Speed Imaging in Biomedical Microfluidic Applications: Principles & Overview. https://www.phantomhighspeed.com/-/media/project/ameteksxa/visionresearch/documents/whitepapers/english/web/wwpmicrobiomed.pdf?la=en&revision=edbcf8a8-2beb-

41dc-a395-00c7473db74a&hash=EEE70F582095C75984E166C1BFC17D56 (accessed April 2022).
(54) Application Notes for Polymer Microparticle Synthesis. https://www.dolomite-microfluidics.com/applications/polymer-microparticle-synthesis/ (accessed Jan 2022).
(55) Atherton, T. J.; Kerbyson, D. J. Size invariant circle detection. *Image and Vision Computing* **1999**, *17* (11), 795−803.
(56) Yuen, H. K.; Princen, J.; Illingworth, J.; Kittler, J. Comparative study of Hough Transform methods for circle finding. *Image and Vision Computing* **1990**, *8* (1), 71−77.
(57) Davies, E. R. Chapter 10: Circle Detection. In *Machine Vision*, 3rd ed.; Davies, E. R., Ed.; Morgan Kaufmann: Burlington, 2005; pp 283−313; DOI: 10.1016/B978-012206093-9/50013-7.
(58) Shao, T.; Bai, L.; Yan, B.; Jin, Y.; Cheng, Y. Modeling the solidification of O/W-emulsion droplet in solvent evaporation technique. *Chem. Eng. Res. Des.* **2017**, *122*, 233−242.
(59) Ku, K. H.; Shin, J. M.; Yun, H.; Yi, G.-R.; Jang, S. G.; Kim, B. J. Multidimensional Design of Anisotropic Polymer Particles from Solvent-Evaporative Emulsion. *Adv. Funct. Mater.* **2018**, *28* (42), 1802961.
(60) Katou, H.; Wandrey, A. J.; Gander, B. Kinetics of solvent extraction/evaporation process for PLGA microparticle fabrication. *Int. J. Pharm.* **2008**, *364* (1), 45−53.

https://doi.org/10.1021/acsbiomaterials.2c00066
ACS Biomater. Sci. Eng. 2022, 8, 2864−2877